I.P.N. - 91406 ORSAY CEDEX

institut de physique nucléaire CNRS - IN2P3 UNIVERSITE PARIS - SUD

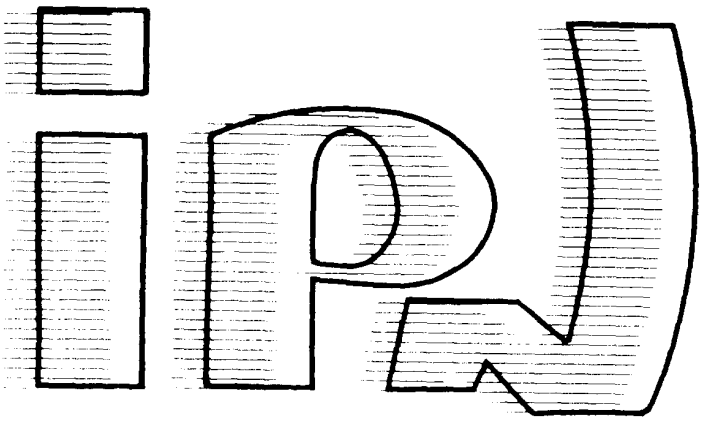

IPNO-DRE 94-02

(Accepted for publication in Physical Review C)

^{29}Si$(d,^3He)^{28}$Al reaction at 29 MeV.

J.Vernotte [1)], G.Berrier-Ronsin [1)], S.Fortier [1)], E.Hourani [1)], J.Kalifa [1)], A.Khendriche [1,2)], J.M.Maison [1)], L.H.Rosier [1)], et G.Rotbard [1)].

1) Institut de Physique Nucléaire, IN2P3-CNRS, B.P.1 91406 Orsay Cedex, France
2) Université de Tizi-Ouzou, Tizi-Ouzou, Algérie

^{29}Si(d, ^3He)^{28}Al reaction at 29 MeV.

J.Vernotte, G.Berrier-Ronsin, S.Fortier, E.Hourani, J.Kalifa,

A.Khendriche*, J.M.Maison, L.H.Rosier, and G.Rotbard

Institut de Physique Nucléaire, Institut National de Physique Nucléaire et de Physique des Particules-Centre National de la Recherche Scientifique, 91406 Orsay Cedex, France

Abstract

The ^{29}Si(d, ^3He)^{28}Al reaction has been investigated at 29 MeV incident energy. Observations using a split-pole magnetic spectrograph have been made of 55 levels of ^{28}Al in the range of excitation energy between 0 and 6.7 MeV. Most of them have been identified with ^{28}Al levels which have been previously observed by other techniques. The spectroscopic factors have been obtained for 23 of these levels through distorted-wave Born approximation (DWBA) analyses of measured angular distributions. The levels at E_x=3.105 and 3.762 MeV have been definitely assigned $J^\pi=1^+$ and 0^+, respectively. Four levels which are populated through the pick-up of a l_p=1 proton have been observed at E_x=4.998, 5.406, 6.021 and 6.652 MeV. The excitation energies and spectroscopic factors for positive-parity states were compared with the results of a recent, complete *sd*-shell space, shell-model calculation. This comparison led to the identification of 21 shell-model levels with experimental levels. This comparison seems accurate enough to make very likely the $J^\pi=3^+$ assignment for the levels at E_x=2.988 and 4.597 MeV which were previously assigned

$J^{\pi}=(1,3)^{+}$.

PACS number(s): 21.10.Hw, 24.10.Eq, 25.40.Hs, 27.30.+t

I. INTRODUCTION.

Shell-model calculations have been done recently for *sd*-shell nuclei by using an effective interaction valid for the complete *sd*-shell space [1]. Many spectroscopic features of the nuclear levels can be predicted from the wavefunctions which are thus obtained and the comparison of the shell-model predictions with experimental results for as many nuclear levels as possible is a necessary step to check the extent of the validity of these calculations.

In particular, shell-model predictions for excitation energies and spectroscopic factors of positive parity states populated through one-nucleon transfer reactions are now available [2]. A comparison of these predictions with experimental results was successfully done for 20 levels with $E_x \leq 9$ MeV populated through the one-proton stripping ^{30}Si($^3He, d$)^{31}P reaction at $E_{^3He}$=25 MeV [3]. Another study of the ($^3He, d$) reaction at the same energy was done also on 17 *sd*-shell target nuclei [4] but, for each of these target nuclei, the study was restricted to a small number (1 to 5) of strongly excited final states. The comparison of the same quantities was also undertaken in the case of the one-proton pickup reaction. For instance, twenty-four ^{26}Mg levels with $E_x \leq 9$ MeV were thus identified with shell-model predicted levels in a recent study of the ^{27}Al(d, ^3He)^{26}Mg reaction at E_d=29 MeV [5].

It seems important to extend this kind of comparison to other *sd*-shell nuclei. So, this paper presents the results obtained for ^{28}Al in a study of the ^{29}Si(d, ^3He)^{28}Al reaction at E_d=29 MeV. This final nucleus was chosen because the present experimental proton pickup spectroscopic information for ^{28}Al is scarce. The only previous study of the ^{29}Si(d, ^3He)^{28}Al reaction was done several years ago at a deuteron energy of 52 MeV [6]. It led to the observation of eleven levels up to $E_x \sim 5$ MeV, one of them (E_x=5.05 MeV) being attributed to the removal of the proton from the 1p shell. Furthermore, it was deduced from the DWBA analysis of the experimental angular distributions that the sum-rule limit of French and Macfarlane [7] was almost completely exhausted by the spectroscopic strengths of the l_p=0 and l_p=2 transitions to the other ten levels. However, an accurate comparison of these experimental results with the shell-model predictions is not possible because the energy resolution

(ΔE$\approx$80-100 keV) does not allow to determine unambiguously which of the many levels known in this odd-odd nucleus [8] contribute actually to the population of the experimental peaks.

Therefore, the first goal of the present work was to try to get such an unambiguous determination from experimental spectra obtained with a good energy resolution by taking advantage of the conjunction of a tandem accelerator and of a split-pole magnetic spectrograph. A second motivation was to search for levels populated through the pickup of a l_p=1 proton and to make an accurate determination of their excitation energy.

II. EXPERIMENTAL PROCEDURE.

A 29 MeV deuteron beam from the upgraded Orsay MP Tandem Van de Graaff accelerator was focused onto a target placed at the center of a scattering chamber, with the beam then being stopped in a graphite Faraday cup connected to a current integrator. The silicon target was prepared by *in vacuo* evaporation of isotopically enriched silicon dioxide onto a carbon backing ($\sim$5 μg-cm^{-2} thick). The method used to determine the target thickness and the enrichment in ^{29}Si will be presented in subsection V.A.

The ^3He particles were momentum analyzed with an Enge split-pole magnetic spectrograph. The detection system has been described previously [3]. The spectrograph horizontal entrance aperture was set to $\pm$1.5^o, which leads to a solid angle $\Omega \simeq$1.6 msr. The angular distribution measurements were done by taking spectra at 6^o and at nine other angles ranging from 9^o to 41^o by steps of 4^o in the laboratory system. The charge Q accumulated during each measurement was equal to 1500 μC from 6^o to 25^o and to 2000 μC for the other four angles. No monitor detector was employed. So, the beam intensity was kept below 250 nA to avoid any deterioration of the target. The constancy of the target thickness was checked by taking two spectra at the same angle (θ_{lab}=13^o) once at the beginning and once at the end of the angular distribution measurements. These two measurements are in excellent agreement.

In order to get the excitation energies, two ^3He spectra were measured at θ_{lab}=10° and 18° in a separate run with the same target and the same solid angle for the spectrograph. The accumulated charge Q was equal to 1700 and 2000 μC, respectively, for these two angles. The spectrum obtained at θ_{lab}=10° and a part of the spectrum obtained at θ_{lab}=18° are displayed in the Figures 1 and 2, respectively. Besides the peaks which are due to the population of levels in ^{28}Al some peaks were identified from their position in the spectra and from their angular distribution with peaks due to the (d, ^3He) reaction on the ^{12}C, ^{13}C, ^{14}N, ^{16}O, ^{28}Si and ^{30}Si nuclei. The full width at half maximum was about 22 keV for all the peaks.

III. ANALYSIS OF SPECTRA AND EXTRACTION OF EXCITATION ENERGIES.

In order to extract the focal plane positions and integrated counts of the individual peaks in the experimental spectra, they were analyzed with the multipeak-fitting code PICOTO [9], a modified version of the code AUTOFIT [10] adapted to the VAX 6000-510 computer of the Institute. Special attention was paid to verifying that the final results obtained from the computer analysis were not dependent upon the initial conditions (values of peak positions and shapes of reference peaks) which were used. Each of the few peaks for which this criterion was not fulfilled will be considered later in Section V.

Absolute cross sections for the (d, ^3He) reaction on the three silicon isotopes were obtained at each angle from the integrated counts in each peak by using the values of the areal densities corresponding to each of these isotopes (and which will be determined in subsection V.A) and by taking into account the integrated charge and the known value of the spectrograph solid angle. The accuracy assigned to these cross sections is obtained by combining the uncertainties in the target thickness (~5% for the number of ^{29}Si nuclei), the solid angle (~4%) and the integrated charge (~1%) with the one arising from the statistics.

Excitation energies were determined from the peak positions of the two spectra at

θ_{lab}=10° and 18°. These two spectra were measured in the same run as the spectra of the ^{27}Al(d, ^3He)^{26}Mg reaction [5] with the same tuning of the detection system so that the same relationship between the radius of curvature of the ^3He-particle's trajectory in the spectrograph and the corresponding peak position in the counter could be used. The peaks from the ^{29}Si(d, ^3He)^{28}Al reaction are clearly apparent at both angles for the levels up to E_x ~3.5 MeV but it is not the case for the levels with E_x >3.5 MeV because some peaks are obscured at either of the two angles by strongly populated peaks from the (d, ^3He) reaction on ^{12}C and ^{16}O. Furthermore the analysis with the code PICOTO is more difficult in this energy region where the level density is increasing and where many peaks are populated only weakly. So, the following criterion was adopted in the E_x >3.5 MeV energy region: only the peaks which appear in at least one of the two spectra at θ_{lab}=10° and 18° and in at least two of the ten angular distribution spectra were taken into account for the determination of the excitation energies. Finally a total number of 55 peaks were considered and excitation energy values were obtained with an accuracy of ±5 keV up to about 6.7 MeV. These values are presented in Table I (column 3) and compared there with the set of values from Ref. [8] (column 1). Most of these values are in agreement within the error limits and the excitation energy values of Ref. [8] were accordingly adopted in the remainder of this paper whenever the error is less than 5 keV in Ref. [8]. The C^2S values which are also presented in Table I (columns 5 to 7) are from the DWBA analysis of the experimental angular distributions measured in this work. This DWBA analysis will be discussed in Section IV. The C^2S values from the previous study of this reaction [6] are also presented for comparison in Table I (columns 8 to 10).

The levels at E_x=3.601, 4.998, 5.406, 6.021 and 6.652 MeV are presented in column 3 as new ^{28}Al levels. The level E_x=3.601 MeV is not identified with the level at E_x=3.591 MeV of Ref. [8] only because the excitation energies are not in agreement within the error limits. As to the other four levels they will be discussed later in subsection V.C. The five peaks observed at E_x=1.624, 5.335, 6.066, 6.451 and 6.489 MeV (column 3) may correspond to the population of several levels of Ref. [8]. The peaks corresponding to the population of

the ^{28}Al level at E_x=2.272 MeV and of the ^{27}Al levels at E_x=2.982 and 3.004 MeV cannot be resolved at any angle of the angular range θ_{lab}=6°-41°. The peaks corresponding to the population of the ^{28}Al levels at E_x=3.296 and 3.671 MeV are also mixed at all angles with the peaks due to the population of the ^{27}Al levels at E_x=4.055 and 4.410 MeV. The last two groups of levels will be considered later in subsection V.B. Two special points are presented below.

The level at E_x=2.566 MeV was reported only in a study of the ^{27}Al$(n,\gamma)^{28}$Al reaction [11]. It was weakly excited and the primary γ-ray was unobserved. A measurable population of this level in the present work would result in a broadening of the peak due to the level at E_x=2.582 MeV. Such a broadening could not be observed at any angle, so the existence of the level at E_x=2.566 MeV cannot be confirmed in this work. The question of the existence of this level will be considered again in subsection V.B.

The level at E_x=3.762 MeV was first observed in the ^{27}Al$(d,p)^{28}$Al reaction [12] as a very weakly populated peak. This level is also populated with a very low cross section (<4μb/sr at θ_{lab}=175°) in the ^{30}Si$(\vec{d},\alpha)^{28}$Al reaction [13]. In the present work, the peak due to the population of this level is hidden at θ_{lab}=10° by the strongly populated peak from the ^{12}C$(d,\ ^3He)^{11}$B(g.s.) reaction but it is clearly apparent at θ_{lab}=18° (Figure 2).

IV. ANALYSIS OF ANGULAR DISTRIBUTIONS

The experimentally measured angular distributions of the $(d,\ ^3He)$ reaction on the various silicon isotopes are analyzed by comparisons with the results of DWBA calculations done with the code DWUCK4 [14]. Spectroscopic factors S_{lj} are extracted from the relationship

$$\left(\frac{d\sigma(\theta)}{d\omega}\right)_{exp} = 2.95\ \frac{C^2 S_{lj}}{(2j+1)}\left(\frac{d\sigma_{lj}(\theta)}{d\omega}\right)_{DWUCK4} \qquad (1)$$

where 2.95 is the normalization factor for the $(d,\ ^3He)$ reaction [15] and S_{lj} is the spectroscopic factor for the pickup of a single proton of orbital angular momentum l and total angular momentum j. The isospin Clebsch-Gordan coefficient C^2 is equal to 1/2, 2/3 and 3/4 for the ^{28}Si, ^{29}Si and ^{30}Si target nuclei, respectively.

The optical parameter sets used for the DWBA analysis are presented in Table II. The deuteron optical set is adapted to the ^{29}Si nucleus from the relationships labelled "79 DCV, L" in Ref. [16]. These relationships result from a global analysis of a large number of elastic scattering and polarization data obtained in many studies at various deuteron energies ranging from 12 to 90 MeV. The same set is adopted for all the silicon isotopes because the differences (which affect only V and a_i) are very small. The ^3He optical parameter set is from the analysis [17] of 25 MeV ^3He elastic scattering from ^{27}Al. It is used for the three aluminum final nuclei. Optical parameter sets with the same origin were used recently for analyzing a study of the ^{27}Al(d, ^3He)^{26}Mg reaction at the same energy [5] and several studies of the ($^3He, d$) reaction on various *sd*-shell nuclei at $E_{^3He}$=25 MeV [3], [4]. The DWUCK4 cross sections are very sensitive to the values of the geometrical parameters of the bound-state potential. The standard values r_o=1.25 fm and a_o=0.65 fm were adopted for this analysis. On the other hand, it has been shown in the case of the ($^3He, d$) reaction [4] that a reduction of the geometrical parameters of the spin-orbit part from the conventional values $r_{s.o.}$=1.25 fm and $a_{s.o.}$=0.65 fm to $r_{s.o.}$=1.00 fm and $a_{s.o.}$=0.52 fm led to a better agreement between the experimental and shell-model spectroscopic factor values for the $1d_{5/2}$ and $1d_{3/2}$ transitions in the entire *sd*-shell. In the present work calculations were done with DWUCK4 by using the conventional values of the geometrical parameters as well as the new ones. These new values led to a decrease of the cross sections (and therefore to an increase of the value of the extracted spectroscopic factors) for the j=l_p+1/2 transitions and to an increase of the cross sections for the j=l_p−1/2 transitions. The decrease and the increase of the cross sections are 18% and 25% for the $1d_{5/2}$ and $1d_{3/2}$ transitions, respectively, in the E_x=0-5 MeV excitation energy range and 8% and 14% for the $1p_{3/2}$ and $1p_{1/2}$ transitions, respectively, in the E_x=5-7 MeV excitation energy range. As in Ref. [5] the DWBA calculations were done in the local and zero-range approximations.

The experimental angular distributions are presented along with the DWUCK4 calculations in the Figure 3 for the ^{28,30}Si(d, ^3He)^{27,29}Al reactions. They are presented in the Figure 4 (l_p=0 and 2 transitions), Figure 5 (l_p=0+2 transitions) and Figure 6 (l_p=1 tran-

sitions) for the ^{29}Si(d, ^3He)^{28}Al reaction. Some experimental angular distributions which could not be fitted by the DWBA calculations are presented in the Figure 7.

It can be seen in the Figure 4 that the first maximum of the experimental angular distributions of the two strong l_p=2 transitions to the ground-state doublet is correctly described by the DWUCK4 calculations. Similarly the amplitudes of the first three oscillations of the strong pure l_p=0 transition to the level at E_x=0.972 MeV, J^π=0^+, are correctly accounted for, but there is a small angular shift (1-2^o) between the calculated and experimental positions of the second and third maxima. A similar angular shift is observed also for the strong l_p=1 transition to the level at E_x=4.998 MeV (Figure 6). The sensitivity of the analysis to the choice of the optical parameters was investigated by doing DWUCK4 calculations for the transitions to the levels at E_x=0, 0.972 and 4.998 MeV with other combinations of deuteron and ^3He optical parameter sets. The deuteron parameters were adapted to the ^{29}Si nucleus and to the incident energy E_d=29 MeV from other relationships obtained also from global analyses of deuteron elastic scattering [18], [19], [20]. The ^3He parameters include a set obtained in Ref. [17] for ^{28}Si (and belonging to the "deep" family as the one of Table II) and two sets used in Refs. [21] and [6] for the analysis of the (d, ^3He) reaction on ^{28}Si and ^{29}Si, respectively. These new optical parameter sets were combined together and with the parameters of Table II. Whatever be the combination of deuteron and ^3He optical parameter sets, quite similar cross sections (within $\pm$8%) are obtained for the l_p=1 and 2 transitions and the same angular shift remains for the l_p=1 transition. As to the l_p=0 transition, the first three oscillations are accounted for best with the parameter combination of Table II.

The C^2S values were obtained by adjusting the first two oscillations of the l_p=0 transitions and the first maximum of the l_p=1 and 2 transitions to the experimental data. In the case of the ^{28}Si and ^{30}Si target nuclei (J^π=0^+), the final levels are populated through pure nlj transitions. In the case of the ^{29}Si target nucleus (J^π=$1/2^+$), the J^π=0^+ and 3^+ final levels are populated also through pure $2s_{1/2}$ and $1d_{5/2}$ transitions, respectively, whereas the J^π=1^+ and J^π=2^+ final levels can involve a mixture of $2s_{1/2}$+$1d_{3/2}$ and $1d_{3/2}$+$1d_{5/2}$ transitions, respectively. Similarly, in the case of the l_p=1 proton pickup, the J^π=0^- and 2^- levels are

populated through pure $1p_{1/2}$ and $1p_{3/2}$ transitions, respectively, whereas a $J^\pi=1^-$ level can involve a mixture of $1p_{1/2}+1p_{3/2}$ transitions. Very similar shapes are predicted in the DWBA calculations for the $j=l_p\pm1/2$ transitions, so that they cannot be distinguished on the basis of the angular distribution measurements of the present work. The C^2S values of the ^{28}Al levels were extracted with the assumption of a $1p_{1/2}$ transfer for the $l_p=1$ transitions and of a $1d_{5/2}$ transfer for the $l_p=2$ transitions (with the exception of the $J^\pi=1^+$ states and of the $J^\pi=2^+$ levels at E_x=3.347 and 3.709 MeV which will be identified in subsection V.B with shell-model states populated through a major $1d_{3/2}$ proton pickup). For levels with excitation energy between 5 and 7 MeV, it has been checked that the relationship

$$\frac{d\sigma_{1p_{3/2}}(\theta)}{d\omega}_{DWUCK4} = 2.38 \frac{d\sigma_{1p_{1/2}}(\theta)}{d\omega}_{DWUCK4} \quad (2)$$

is valid within 7% in the angular range $\theta_{lab}=6^o-21^o$ used to extract the C^2S values. Similarly, the relationship

$$\frac{d\sigma_{1d_{5/2}}(\theta)}{d\omega}_{DWUCK4} = 2.15 \frac{d\sigma_{1d_{3/2}}(\theta)}{d\omega}_{DWUCK4} \quad (3)$$

is valid within 10% in the ranges $\theta_{lab}=9^o-24^o$ and E_x=1.5-5 MeV. It follows that the relationships $S_{1d_{5/2}} \approx 0.70\ S_{1d_{3/2}}$ and $S_{1p_{3/2}} \approx 0.84\ S_{1p_{1/2}}$ hold for all the ^{28}Al states in the excitation energy range of this work.

In a conservative way the uncertainties of the DWBA analysis are estimated to contribute a 20% systematic uncertainty to the spectroscopic factors of the most strongly populated levels. This uncertainty can be larger in the case of the weakly populated levels which have poor statistics and for which the single-step reaction model might be a poor approximation. The C^2S values obtained with the parameters of Table II (and with the conventional values $r_{s.o.}$=1.25 fm and $a_{s.o.}$=0.65 fm for the spin-orbit part of the form factor) are presented in Table I (columns 5 to 7) for the ^{28}Al levels and in Table III (column 4) for some ^{27}Al levels. The choice of the conventional geometrical parameters was made in order to allow a more direct comparison with the spectroscopic factor values obtained by other authors. It can be seen in Table I that the C^2S values obtained for the $l_p=0$ and 2 transitions in Ref. [6] are

generally in good agreement with the values of the present work. In particular it is worth pointing out that this agreement is good between the C^2S values obtained in Ref. [6] for the complex peaks at E_x=0, 0.99 and 2.21 MeV and the sum of the C^2S values obtained in this work for the resolved components. The difference between the C^2S values for the l_p=1 state at E_x ~5 MeV will be considered later in subsection V.C.

As it will be explained in subsection V.A, the transition to the ground state of ^{27}Al was analyzed in the present work by assuming a value of C^2S equal to the mean value of the ones of the Refs. [21] and [6]. Because of this choice, the C^2S values of the other ^{27}Al levels considered in this work are expected to be in agreement with the values of the Refs. [21] and [6]. This is indeed the case (Table III) with the exception of the l_p=0 transition, the C^2S value of which is larger in the present work. The shell-model predicted C^2S values for the positive parity levels [2] are also presented in Table III.

For the transitions to the seven ^{28}Al levels with known (or possible) $J^\pi=1^+$ values [8], the relative strengths of the two spectroscopic factors were searched for by minimizing the quantity

$$D^2 = \sum_{i=1}^{N} \left(\frac{\sigma_{i,\ exp} - \sigma_{i,\ DWBA}}{\Delta\sigma_{i,\ exp}} \right)^2 \tag{4}$$

where N is the number of angles considered in the sum and $\sigma_{i,\ DWBA}$ stands for

$$2.95\ C^2S_{0+2} \left(\frac{d\sigma_i(\theta)}{d\omega} \right)_{DWBA} \text{ and}$$

$$C^2S_{0+2} \left(\frac{d\sigma(\theta)}{d\omega} \right)_{DWBA} =$$

$$C^2S_{0+2} \left\{ \frac{\alpha}{2} \left(\frac{d\sigma_{2s_{1/2}}(\theta)}{d\omega} \right)_{DWUCK4} + \frac{(1-\alpha)}{4} \left(\frac{d\sigma_{1d_{3/2}}(\theta)}{d\omega} \right)_{DWUCK4} \right\} \tag{5}$$

where α is the weight of the l_p=0 transition. The search for α was restricted to the five forward angles which are fairly enough accounted for in the case of pure transitions. The value of α thus obtained yields the values $C^2S_0 = \alpha\ C^2S_{0+2}$ and $C^2S_2 = (1-\alpha)\ C^2S_{0+2}$. It is difficult to estimate the imprecision $\Delta\alpha$ which is attached to the value of α. In this analysis this imprecision has been estimated somewhat arbitrarily as equal to the difference between the values of α leading to D^2_{min} and $D^2 = 2D^2_{min}$.

The analysis is more sensitive to the presence of a weak $2s_{1/2}$ transition in a dominant $1d_{3/2}$ transition than to the reverse situation because, at the two forward angles, the DWUCK4 cross sections are larger for the $2s_{1/2}$ than for the $1d_{3/2}$ transitions by factors of 10 and 3, respectively. A change in the shape of a dominant l_p=2 transition can thus be observed for values of α as low as 0.03. A transition has been considered as a pure transition if the value of D^2 obtained for α=0.00 or α=1.00 is smaller than $2D^2_{min}$. It was the case for the transitions to the level at E_x=1.373 MeV (pure l_p=0 transition) and to the levels at E_x=1.620 and 2.201 MeV (pure l_p=2 transitions). Therefore, the corresponding experimental and DWUCK4 angular distributions are presented in the Figure 4 with the other pure transitions. However, it has to be pointed out that the level at E_x=1.620 MeV could not be resolved from the level at E_x=1.623 MeV, $J^\pi=2^+$. So, the weight of the l_p=2 transition obtained from the analysis of the angular distribution of the experimental peak can be overestimated since the level at E_x=1.623 MeV is populated through a pure l_p=2 transition. The experimental and DWUCK4 angular distributions of the other mixed transitions are presented in the Figure 5. The values of α are 0.04±0.01, 0.57±0.05, 0.32±0.08 and 0.13±0.06 for the levels at E_x=3.105, 3.542, 4.115 and 4.846 MeV, respectively. For the corresponding C^2S values, an additional imprecision which can be as large as 35% follows from the imprecision in the determination of α.

V. DISCUSSION.

A. Determination of the silicon target thickness and of the enrichment in ^{29}Si.

The strongly excited peaks due to the ^{28}Si(d, ^3He)^{27}Al reaction which are observed in the Figure 1 are the indication of the presence of an important amount of ^{28}Si in the target. On the other hand the weak excitation of the peak due to the population of the ^{29}Al ground state which is known to be strongly populated in the ^{30}Si(d, ^3He)^{29}Al reaction through a $1d_{5/2}$ transition [6] gives evidence for the presence of a small amount of ^{30}Si. The number

of ^{28}Si and ^{30}Si nuclei were estimated in the following way.

The ^{28}Si(d, ^3He)^{27}Al reaction has been studied several times previously [6,21–23] and the C^{2}S values obtained by the various authors for the strong $1d_{5/2}$ transition to the ground state vary from 2.30 [22] up to 3.75 [21]. In this work the experimental angular distribution of the ^{27}Al ground state transition was analyzed with the assumption of a C^{2}S value equal to 3.57 which is the mean value of the Refs. [6] and [21] (C^{2}S=3.40 and 3.75, respectively). This choice was made because these two values are close to the shell-model value C^{2}S=3.62 [2]. This assumption involves the presence in the target of an amount of ^{28}Si equal to $\mathcal{N}(^{28}\text{Si})=1.30\times10^{17}$ nuclei-cm^{-2}. Similarly, the value $\mathcal{N}(^{30}\text{Si})=0.058\times10^{17}$ nuclei-cm^{-2} is obtained from the analysis of the $1d_{5/2}$ ground-state transition in the ^{30}Si(d, ^3He)^{29}Al reaction with the assumption of a spectroscopic factor equal to the one of Ref. [6] (C^{2}S=3.96) which is very close to the shell-model predicted value C^{2}S=3.80 [2].

The number of ^{29}Si nuclei in the target was then obtained from the elastic scattering measurements of 29 MeV deuterons from the same target at 7 angles in the region of the second maximum of the angular distribution (θ_{lab}=25^o, 27^o, 28^o, 29^o, 30^o, 31^o and 33^o). The peaks from the three silicon isotopes are not experimentally resolved at these angles. However, since the spectrograph solid angle and the integrated charge for each of the measurements are known, the number of ^{29}Si nuclei can be calculated at each angle from the number of counts in the elastic peak by taking into account the quoted above number of ^{28}Si and ^{30}Si nuclei and by using the elastic scattering cross sections obtained from the DWUCK4 calculations. Each of these seven determinations differs by less than 5% from the mean value $\mathcal{N}(^{29}\text{Si})=11.3\times10^{17}$ nuclei-cm^{-2}. The number of nuclei for the three silicon isotopes lead to a target thickness of 60$\pm$3 μg-cm^{-2} (with an enrichment of 90% in ^{29}Si, about 10% in ^{28}Si and <1% in ^{30}Si). It is worth pointing out that the choice of another C^{2}S value for the ^{27}Al ground-state transition leads to a much larger relative change in the number of ^{28}Si nuclei than in the number of ^{29}Si nuclei. For instance, the choice of the smallest value, C^{2}S=2.30 [22], leads to $\mathcal{N}(^{28}\text{Si})=2.00\times10^{17}$ nuclei-cm^{-2} and to $\mathcal{N}(^{29}\text{Si})=10.7\times10^{17}$ nuclei-cm^{-2}. This value remains in agreement within 5% with the value $\mathcal{N}(^{29}\text{Si})=11.3\times10^{17}$

nuclei-cm^{-2}, so that the method which has been used to get the number $\mathcal{N}(^{29}\mathrm{Si})$ can be considered as reasonably precise.

B. Comparison between experimental and shell-model excitation energies and C^2S values for positive-parity ^{28}Al states.

Excitation energies and one-proton pickup spectroscopic factors have been calculated in the framework of the shell-model [2] for the ^{28}Al levels which are populated through the $2s_{1/2}$, $1d_{3/2}$ and $1d_{5/2}$ transitions. The total spectroscopic strengths ΣC^2S calculated for all the positive-parity states with $J^\pi \leq 3^+$ amounts to 4.894, 0.586 and 0.519 for the $1d_{5/2}$, $2s_{1/2}$ and $1d_{3/2}$ transitions, respectively. The results of the calculations are presented in Table IV, columns 1 to 5, for the first six levels with $J^\pi=0^+$ and for the first eight levels with each of $J^\pi=1^+$, 2^+ and 3^+. Twenty-six of these thirty levels have excitation energies below $\sim$5 MeV and carry 90% of the total calculated spectroscopic strengths. Since this excitation energy range has been carefully investigated in the present work, an extensive comparison between the experimental results and the shell-model predictions can be undertaken. The identification between experimental and shell-model predicted levels is based upon the similarity of the excitation energies and C^2S values (and upon the identity of the J^π-values when they are known for the experimental levels). However, it can be observed in Table IV that the spectroscopic strengths are very unequally distributed among the shell-model states. In particular, more than 75% of the total spectroscopic strengths calculated for the $1d_{5/2}$ and $2s_{1/2}$ transitions are concentrated upon the first two levels populated through these transitions and the highest-lying shell-model state with a C^2S value larger than or equal to 0.1 is the $J^\pi=2^+_5$ level at 3.135 MeV. The identification of experimental and shell-model levels based on the similarity of the C^2S values is thus expected to be more difficult above E_x $\sim$3 MeV because, as indicated in Section IV, a larger imprecision is expected for the spectroscopic factors of weakly populated levels. Likewise, the identification based on the similarity of the excitation energies can be complicated above E_x $\sim$3 MeV because the level density is

increasing in this odd-odd nucleus.

There is an additional difficulty for the $J^{\pi}=2^{+}$ levels which can be populated through $1d_{5/2}$ and $1d_{3/2}$ transitions with the same DWBA shapes as was pointed out in Section IV. For an incoherent sum of $1d_{3/2}$ and $1d_{5/2}$ contributions the calculated C^2S_{sm} value to be compared with the experimental one is obtained as following. By using the relationship (1) the calculated cross section can be written

$$\left(\frac{d\sigma(\theta)}{d\omega}\right)_{calc} = 2.95\ C^2 \left\{ \frac{S_{sm}(d_{3/2})}{4} \left(\frac{d\sigma_{d_{3/2}}(\theta)}{d\omega}\right)_{DWUCK4} + \frac{S_{sm}(d_{5/2})}{6} \left(\frac{d\sigma_{d_{5/2}}(\theta)}{d\omega}\right)_{DWUCK4} \right\} \quad (6)$$

By taking into account the relationship (3), the relationship (6) becomes

$$\left(\frac{d\sigma(\theta)}{d\omega}\right)_{calc} = 2.95\ \frac{C^2}{6} \left(\frac{d\sigma_{d_{5/2}}(\theta)}{d\omega}\right)_{DWUCK4} \left(S_{sm}(d_{5/2}) + 0.70\ S_{sm}(d_{3/2})\right) \quad (7)$$

or

$$\left(\frac{d\sigma(\theta)}{d\omega}\right)_{calc} = 2.95\ \frac{C^2}{4} \left(\frac{d\sigma_{d_{3/2}}(\theta)}{d\omega}\right)_{DWUCK4} \left(S_{sm}(d_{3/2}) + 1.43\ S_{sm}(d_{5/2})\right) \quad (8)$$

The calculated C^2S_{sm} values presented in the column 6 of Table IV are then obtained from the relationship (7) if the experimental angular distribution is analyzed with the assumption of a dominant $1d_{5/2}$ transfer and from the relationship (8) in the other case (which concerns only the transitions to the levels at E_x=3.447 and 3.709 MeV as indicated in Section IV).

The excitation energies, J^{π}-values and C^2S values of the experimental levels which are identified with the shell-model predicted ones are presented in Table IV, columns 7 to 10, and the difference between the experimental and shell-model excitation energies is presented in the column 11. A graphical presentation of this comparison is displayed in the Figure 8.

With the exception of the level at E_x=2.566 MeV, all the levels with $J^{\pi} \leq 3^{+}$ and E_x <3.5 MeV listed in Ref. [8] have been thus identified easily enough with shell-model predicted levels. The following comments can be made. The experimental and shell-model C^2S values are in a nice agreement for the levels with $J^{\pi}=0^{+}_{1}$, 1^{+}_{1}, 2^{+}_{1} and 3^{+}_{1} but there is an inversion in the order of the members of the ground-state doublet. For the other levels populated through a pure (or dominant) l_p=2 transition, the experimental C^2S values are larger by a

factor which can be as high as 3 (for the levels at E_x=1.014 and 2.486 MeV). This factor is even about 4 for the level at E_x=3.296 MeV but a larger imprecision cannot be excluded for the experimental value. The level at E_x=3.296 MeV is indeed mixed at all angles with the ^{27}Al level at E_x=4.055 MeV, $J^\pi=1/2^-$, as it was pointed out in Section III. The two contributions obtained from the code PICOTO were found to be dependent on the initial conditions. So, for each of the experimental spectra, the total number of counts due to the population of the two levels was considered to get the experimental angular distribution which was then analyzed by adapting the relationship (5) to the case of the $1p_{1/2}$ and $1d_{5/2}$ transitions in the $(d, {}^3He)$ reactions on ^{28}Si and ^{29}Si, respectively. The weight α of the l_p=1 transition was searched for by considering only the experimental points at θ_{lab}=9°, 13°, 17° and 21° which are correctly described for both of the transitions. The best fit (Figure 3) is obtained for α=0.75. By taking into account the DWUCK4 cross sections for the $1p_{1/2}$ and $1d_{5/2}$ transitions, this value indicates a dominant contribution of the ^{27}Al level to the experimental peak (at least at the forward angles).

The similarity of the excitation energies and J^π-values leads to the identification of the two levels at E_x=1.620 and 1.623 MeV with the $J^\pi=1_2^+$ and 2_2^+ shell-model levels at E_x=1.746 and 1.537 MeV, respectively. The peak which is observed at $E_x \sim$1.62 MeV in the Figure 1 is thus attributed to the population of the two levels at E_x=1.620 and 1.623 MeV, because the two shell-model levels are both predicted to be populated in the $(d, {}^3He)$ reaction. The experimental C^2S value is in agreement with the sum of the calculated ones for the $J^\pi=1_2^+$ and 2_2^+ levels. According to the shell-model predictions, the population of the $J^\pi=2^+$ member of the doublet would be dominant.

By considering the similarity of the excitation energies and of the C^2S values, it seems quite reasonable to identify the experimental level at E_x=2.988 MeV with the shell-model level at E_x=3.061 MeV, $J^\pi=3_3^+$, and therefore to restrict the value $J^\pi=(1,3)^+$ of Ref. [8] to $J^\pi=3^+$.

The level at E_x=3.012 MeV was assigned $J^\pi=0^+$ in a study of the ^{30}Si$(\vec{d},\alpha)^{28}$Al reaction [13] at a backward angle (θ_{lab}=175°). It was also reported in various studies of

the ^{27}Al$(d,p)^{28}$Al reaction [12], [24], [25]. In the angular distribution measurements of the present work, it could be observed only at two angles (θ_{lab}=6° and 9°) because, at the other angles, the experimental peak is vanishing in the tail of the much more intense peak due to the population of the level at E_x=2.988 MeV. The observation at the two most forward angles is consistent with the forward peaked shape of the l_p=0 transition populating a $J^\pi=0^+$ level. The experimental value of the C^2S value is presented in parentheses in Tables I and IV because it is obtained from these two measurements only. This very small value is to be compared with C^2S=0.000, the shell-model predicted value for the $J^\pi=0_2^+$ level at E_x=2.895 MeV.

The level at E_x=3.105 MeV is assigned $J^\pi=(1,3)^+$ in Ref. [8]. The increase of the experimental cross section at θ_{lab}=6° (Figure 5) indicates the presence of a weak l_p=0 contribution mixed with a dominant l_p=2 contribution, so that this level can be assigned $J^\pi=1^+$. It is identified with the $J^\pi=1_4^+$ shell-model level though no l_p=2 strength is predicted for this level by the shell-model calculations (Table IV).

It appears then that, in the excitation range below E_x <3.5 MeV, the level at E_x=2.566 MeV, $J^\pi=(1-3^+)$, is the only level which has no correspondent among the shell-model predicted positive parity states. A first conclusion would be that this level is a negative parity state with $J^\pi=(1,2)^-$. The simplest configurations leading to a negative parity state in ^{28}Al are the ones which involve the removal of a nucleon from the $1p$ orbit and the promotion of a nucleon into the $2p$ and/or $1f$ orbits. Now the first fragments of the inner $1p$ configuration and of the $1f$-$2p$ configurations are observed at excitation energies much higher than 2.566 MeV: E_x=4.998 MeV for the $1p$ configuration (see subsection V.C) and E_x=3.465 MeV for the $1f$-$2p$ configurations reached through the (d,p) reaction [12], [25]. The existence of a negative parity state due to a more complicated configuration and lying at a lower excitation energy seems very unlikely. It has also to be pointed out that this level which has been reported only once [11] (see Section III) is considered in Ref. [26] as almost certainly nonexisting.

Some levels with E_x >3.5 MeV are discussed now. The levels at E_x=3.542, 4.115 and

4.846 MeV, $J^\pi=1^+$, and at E_x=4.244 MeV, $J^\pi=2^+$, are identified with the shell-model levels at E_x=3.524, 3.925 and 4.929 MeV, $J^\pi=1^+_5$, 1^+_6 and 1^+_7 and at E_x=4.030 MeV, $J^\pi=2^+_8$, respectively. The differences between the excitation energies are quite consistent with the other values of Table IV. In the case of the mixed transitions leading to the $J^\pi=1^+$ levels, the experimental and shell-model C^2S values are in a fair enough agreement with the exception of the l_p=2 contribution to the level at E_x=4.846 MeV (Table IV). It seems also worth pointing out that the experimental and shell-model values of α are in reasonable agreement for the three levels (Table IV) (even though the experimental values are smaller for the three levels).

The level at E_x=3.671 MeV, $J^\pi=3^+$ [8], could correspond to one of the shell-model levels at E_x=3.474, 3.598 and 3.876 MeV, $J^\pi=3^+_5$, 3^+_6 and 3^+_7, respectively. If this level is populated in this work, the corresponding peak is mixed at all angles with a peak due to the population of the ^{27}Al level at E_x=4.410 MeV, $J^\pi=5/2^+$, as it was pointed out in Section III. By assuming that the experimental peak is due to the population of only one of the two levels, the DWBA analysis leads to upper limits of 0.42 and 0.049 for the C^2S values of the levels of ^{27}Al and ^{28}Al, respectively. The upper limit obtained for the ^{27}Al level must be compared to the C^2S values of 0.29 [6] and 0.35 [21]. So, the population of the ^{28}Al level at E_x=3.671 MeV in the present work does not seem firmly established and, for this reason, this level appears only in parentheses in the Figure 2. The level at E_x=3.709 MeV, $J^\pi=(2,3)^+$, [8] could correspond to one of the shell-model levels at E_x=3.632, 3.715 and 3.876 MeV, $J^\pi=2^+_6$, 2^+_7 and 3^+_7, respectively, but the present experimental results do not allow a more precise identification. However, it has to be pointed out that the levels at E_x=3.671 and 3.709 MeV have been identified in Ref. [26] with the $J^\pi=3^+_5$ and $J^\pi=2^+_6$ shell-model levels at E_x=3.474 and 3.632 MeV, respectively. So, the levels at E_x=3.671 and 3.709 MeV are also presented in Table IV and in Figure 8 even though the identification is not from the present work.

The peak corresponding to the population of the level at E_x=3.762 MeV is obscured at some angles by the much more intense peak from the $^{12}C(d, {}^3He)^{11}B$(g.s.) reaction.

Despite the missing points, the experimental angular distribution is clearly accounted for by a l_p=0 transition (Figure 4). The $J^\pi=0^+$ value which was only suggested from a study of the $^{30}Si(\vec{d},\alpha)^{28}Al$ reaction [13] is thus confirmed. This level is identified with the $J^\pi=0^+_3$ shell-model level at E_x=3.449 MeV. The experimental and shell-model C^2S values are in agreement within a factor of 2.

The level at E_x=4.597 MeV was assigned $J^\pi=1^+$ in Ref. [8] but this assignment has been changed into $J^\pi=(1,3)^+$ in Ref. [26]. This level is then identified with the $J^\pi=3^+_8$ shell-model level at E_x=4.230 MeV. The experimental and shell-model C^2S values are in agreement within a factor of 3. The deviations between the experimental and shell-model excitation energies of the $J^\pi=0^+_3$ and $J^\pi=3^+_8$ levels have the largest values observed in this comparison.

C. ^{28}Al levels populated through l_p=1 transitions.

The experimental angular distributions of the transitions leading to the four levels at E_x=4.998, 5.406, 6.021 and 6.652 MeV are correctly accounted for by DWBA calculations done for l_p=1 transitions (Figure 6). These levels can therefore be assigned $J^\pi=(0-2)^-$. However, as indicated in Section IV, the C^2S values presented in Table I were obtained with the assumption of a $1p_{1/2}$ transition.

The strongly populated level at E_x=4.998 MeV is identified with the l_p=1 level observed at E_x=5.05 MeV in the previous study of the $^{29}Si(d,\,^3He)^{28}Al$ reaction [6]. The level at E_x=4.998 MeV constitutes a close doublet with the level at E_x=4.999 MeV which is assigned $J^\pi=2^+$ in Ref. [8] by considering its population through a mixed l_p=0+2 transition in the $^{27}Al(d,p)^{28}Al$ reaction [25] and the natural parity determined in the $^{30}Si(\vec{d},\alpha)^{28}Al$ reaction [13].

The strongly excited peak which appears in Figure 1 at E_x ~5.4 MeV is due to the population of several levels. The most populated of these levels (E_x=5.406 MeV) is also the only one for which the results from the code PICOTO are not dependent upon the initial

conditions. By considering only the excitation energies, the level at E_x=5.406 MeV and the other two levels populated through l_p=1 transitions and observed at E_x=6.021 and 6.652 MeV could correspond (within error limits) to the three levels of the Ref. [8] at E_x=5.402, 6.020 and 6.651 MeV, respectively. The level at E_x=5.402 MeV was observed only once in the $^{27}Al(d,p)^{28}Al$ reaction [24]. The levels at E_x=6.020 and 6.651 MeV were observed in the $^{27}Al(d,p)^{28}Al$ reaction [24,27] and in the $^{27}Al(n,\gamma)^{28}Al$ reaction [11] and they were assigned $J^\pi=(1^+-4^+)$ and $J^\pi=(0^+-3^+)$, respectively, from their γ-decay schemes [11]. If the three levels at E_x=5.402, 6.020 and 6.651 MeV are the same as the l_p=1 states of the present work they should be populated through l_n=1 transfers in the (d,p) reaction. Unfortunately, this cannot be proved since angular distribution measurements were not done in these (d,p) studies. The identification would lie then only upon the similarity of the excitation energies. Such an identification seemed to us highly speculative at these excitation energies, and the levels at E_x=5.406, 6.021 and 6.652 MeV are therefore presented in Table I as new levels.

It can be thought that the ^{28}Al level at E_x=4.998 MeV is most likely populated through a $1p_{1/2}$ transition since the lowest odd-parity state observed in the $(\vec{d}, {}^3He)$ reaction on the ^{16,18}O, ^{20,22}Ne, ^{24,26}Mg and ^{28}Si even-even nuclei is due to the pickup of a $1p_{1/2}$ proton [28]. The J^π-value would be thus restricted to $(0,1)^-$. The value C^2S=0.77 obtained in this work (Table I) is substantially lower than the value C^2S=1.10 of Ref. [6]. A similar difference between the C^2S values of the l_p=1 transitions at the two energies E_d=29 and 52 MeV was previously pointed out in the case of the $^{27}Al(d, {}^3He)^{26}Mg$ reaction [5].

The assumption of the population of the level at E_x=5.406 MeV through a $1p_{1/2}$ transition seems also the most likely for the following reasons:

1) due to the $J^\pi=1/2^+$ value of the ground state of ^{29}Si, the $1p_{1/2}$ strength is expected to be shared between at least two levels with $J^\pi=0^-$ and 1^-, respectively.

2) the difference between the excitation energies of the two levels at E_x=4.998 and 5.406 MeV is only about 400 keV whereas in the neighbouring nuclei ^{25}Na and ^{27}Al the first two levels carrying a substantial portion of the $1p_{1/2}$ and $1p_{3/2}$ strengths are separated by more than 1 MeV.

The summed C^2S values for the two levels at E_x=4.998 and 5.406 MeV amount to 1.09 (with the assumption of a $1p_{1/2}$ transfer for the two levels). This value is to be compared to the values 1.51 [6] (or 1.80 [21]) for the ^{27}Al level at E_x=4.055 MeV and 2.84 for the ^{25}Na level at E_x=3.995 MeV [29]. However, it must be pointed out that the ^{25}Na value exceeds the sum-rule limit which is equal to 2 for the $1p_{1/2}$ transitions.

From the present work only it is not possible to conclude whether the levels at E_x=6.021 and 6.652 MeV are populated through $1p_{1/2}$ or $1p_{3/2}$ transitions. If further investigations could allow the identification of these levels with the levels at E_x=6.020 and 6.651 MeV of Ref. [8], these levels could then be assigned $J^\pi=2^-$ and $(1,2)^-$, respectively, and the level at E_x=6.020 MeV would be one of the levels among which the $1p_{3/2}$ strength is distributed.

VI. SUMMARY.

The present work provides an accurate determination of the excitation energy of many levels populated in the one-proton pickup reaction on the ^{29}Si nucleus. The level at E_x=3.105 MeV which was previously assigned $J^\pi=(1,3)^+$ has been definitely assigned $J^\pi=1^+$. The previous, tentative $J^\pi=0^+$ assignment to the level at E_x=3.762 MeV is confirmed. Four levels are attributed to the pickup of a proton from the $1p$ shell. Twenty-one of the twenty-six shell-model predicted positive parity levels with $J^\pi \leq 3^+$ and E_x <5 MeV are identified with experimental levels by comparing the experimental and shell-model values for J^π, excitation energies, and C^2S values. This comparison led to the $J^\pi=3^+$ assignment for the levels at E_x=2.988 and 4.597 MeV, respectively, which were previously assigned $J^\pi=(1,3)^+$. This result shows that such a careful comparison can be used as a spectroscopic tool in some cases.

ACKNOWLEDGMENTS

The authors are very grateful to Professor Endt for the communication of Ref. [26] before publication. They are also indebted to R.Marquette for the ^{29}Si target preparation. At last,

they acknowledge the operating crew of the Orsay MP Tandem for the efficient running of the accelerator.

REFERENCES

* Permanent address: *University of Tizi Ouzou, Tizi Ouzou, Algeria.*

[1] B. H. Wildenthal, Progress in Particle and Nuclear Physics, **11**, 5 (1984).

[2] B. H. Wildenthal, private communication.

[3] J. Vernotte, A. Khendriche, G. Berrier-Ronsin, S. Grafeuille, J. Kalifa, G. Rotbard, R. Tamisier, and B. H. Wildenthal, Phys. Rev. **C41**, 1956 (1990).

[4] J. Vernotte, G. Berrier-Ronsin, J. Kalifa, R. Tamisier, and B. H. Wildenthal, to be published in Nuclear Physics.

[5] J. Vernotte, G. Berrier-Ronsin, S. Fortier, E. Hourani, J. Kalifa, J. M. Maison, L. H. Rosier, G. Rotbard, and B. H. Wildenthal, Phys. Rev. **C48**, 205 (1993).

[6] H. Mackh, G. Mairle, and G. J. Wagner, Z. Physik. **269**, 353 (1974).

[7] J. B. French and M. H. Macfarlane, Nucl. Phys. **26** 168 (1961).

[8] P. M. Endt, Nucl. Phys. **A521**, 1 (1990).

[9] P. Picot, Internal Report of Institut de Physique Nucléaire Orsay No. IPNO-T-81-03, Orsay, 1981.

[10] J. R. Comfort, Argonne National Laboratory Physics Division Informal Report Phy-1970 B(unpublished).

[11] H. H. Schmidt, P. Hungerford, H. Daniel, T. von Egidy, S. A. Kerr, R. Brissot, G. Barreau, H. G. Börner, C. Hofmeyr, and K. P. Lieb, Phys.Rev. **C25**, 2888 (1982).

[12] T. P. G. Carola and J. G. van der Baan, Nucl. Phys. **A173**, 414 (1971).

[13] D. O. Boerma, W. Grüebler, V. König, P. A. Schmelzbach, and R. Risler, Nucl.Phys. **A270**, 15 (1976).

[14] P. D. Kunz, private communication.

[15] R. H. Bassel, Phys. Rev. **149**, 791 (1966).

[16] W. W. Daehnick, J. D. Childs, and Z. Vrcelj, Phys. Rev. **C21**, 2253 (1980).

[17] J. Vernotte, G. Berrier-Ronsin, J. Kalifa, and R. Tamisier, Nucl. Phys. **A390**, 285 (1982).

[18] E. Newman, L. C. Becker, B. M. Preedom, and J. C. Hiebert, Nucl. Phys. **A100**, 225 (1967).

[19] F. Hinterberger, G. Mairle, U. Schmidt-Rohr, G. J. Wagner, and P. Turek, Nucl. Phys. **A111**, 265 (1968).

[20] G. Mairle, K. T. Knöpfle, H. Riedesel, G. J. Wagner, V. Bechtold, and L. Friedrich, Nucl. Phys. **A339**, 61 (1980).

[21] B. H. Wildenthal and E. Newman, Phys. Rev. **167**, 1027 (1968).

[22] H. E. Gove, K. H. Purser, J. J. Schwartz, W. P. Alford, and D. Cline, Nucl. Phys. **A116**, 369 (1968).

[23] R. E. Tribble and K. I. Kubo, Nucl. Phys. **A282**, 269 (1977).

[24] W. W. Buechner, M. Mazari, and A. Sperduto, Phys. Rev. **101**, 188 (1956).

[25] S. Chen, J. Rapaport, H. Enge, and W. W. Buechner, Nucl. Phys. **A197**, 97 (1972).

[26] P. M. Endt, and J. G. L. Booten, Nucl. Phys. **A455**, 499 (1993).

[27] L. M. Solin, V. N. Kuzmin, Y. A. Nemilov, and V. A. Kalinin, Yad. Fiz. **43**, 6 (1986).

[28] G. Mairle, G. J. Wagner, K. T. Knöpfle, Liu Ken Pao, H. Riedesel, V. Bechtold, and L. Friedrich, Nucl. Phys. **A363**, 413 (1981).

[29] T. Kihm, G. Mairle, P. Grabmayr, K. T. Knöpfle, G. J. Wagner, V. Bechtold, and L. Friedrich, Z. Phys.A-Atoms and Nuclei **318**, 205 (1984).

FIGURES

FIG. 1. Spectrum of the ^{29}Si(d, ^3He)^{28}Al reaction taken at θ_{lab}=10^o for an accumulated charge of 1700μC. The excitation energies are from Ref.[8]. The peaks which are due to the (d, ^3He) reaction on nuclei other than ^{29}Si are presented with the excitation energy in the corresponding final nucleus. In this spectrum, the peak due to the population of the ^{27}Al ground state is partly truncated by the edge of the counter.

FIG. 2. Part of the spectrum of the ^{29}Si(d, ^3He)^{28}Al reaction taken at θ_{lab}=18^o for an accumulated charge of 2000μC. Some peaks which are hidden in Figure 1 by the strongly populated peak from the ^{12}C(d, ^3He)^{11}B(g.s.) reaction can be observed in this spectrum. For instance, it is the case of the level at E$_x$=3.762 MeV (see text, Section III). The level at E$_x$=3.671 MeV is presented in parentheses because its population in this work is not clearly established (see text, subsection V.B).

FIG. 3. Angular distributions from the ^{28,30}Si(d, ^3He)^{27,29}Al reactions. If not shown, the error is smaller than the point size. The ^{27}Al levels at E$_x$=4.055 and 4.410 MeV cannot be resolved from the ^{28}Al levels at E$_x$=3.296 and 3.671 MeV, respectively. The analysis of these experimental angular distributions was done as indicated in subsection V.B. For the levels at E$_x$=3.296 MeV in ^{28}Al and E$_x$=4.055 MeV in ^{27}Al, the crossed and dashed curves are the cross sections obtained by using the values C^{2}S(3.296 MeV)=0.06 (Table I) and C^{2}S(4.055 MeV)=1.57 (Table III), respectively, and by taking into account the isotopic composition of the silicon target. The continuous curve is the sum of the two contributions. For the level at E$_x$=4.410 MeV, the continuous curve is the fit for C^{2}S(4.410 MeV)=0.42 (Table III).

FIG. 4. Angular distributions from the ^{29}Si(d, ^3He)^{28}Al reaction for the l_p=0 and l_p=2 transitions. If not shown, the error is smaller than the point size. Curves result from DWBA calculations.

FIG. 5. Angular distributions from the ^{29}Si(d, ^3He)^{28}Al reaction for the mixed l_p=0+2 transitions. If not shown, the error is smaller than the point size. Curves result from DWBA calculations. The contributions for the l_p=0 and l_p=2 transitions (dashed and crossed curves, respectively) are weighted by the C^2S values presented in Table I.

FIG. 6. Angular distributions from the ^{29}Si(d, ^3He)^{28}Al reaction for the l_p=1 transitions. If not shown, the error is smaller than the point size. Curves result from DWBA calculations. The presence of the strong peak from the ^{12}C(d, ^3He)^{11}B reaction to the first excited state of ^{11}B at E_x=2.124 MeV prevents the observation of the point at θ_{lab}=17^o in the experimental angular distribution of the transition to the level at E_x=6.021 MeV. Similarly the experimental angular distribution of the transition to the level at E_x=6.652 MeV could be measured only at the six forward angles because of the peak from the ^{16}O(d, ^3He)^{15}N reaction to the third excited state of ^{15}N at E_x=6.324 MeV.

FIG. 7. Angular distributions from the ^{29}Si(d, ^3He)^{28}Al reaction which could not be fitted by DWBA predictions.

FIG. 8. Identification of experimental positive parity levels in ^{28}Al with shell-model predicted levels. This identification is done as explained in text (subsection V.B). The i^{th} shell-model level with the spin J is presented in the column "J, i". For the experimental levels the excitation energies are from Ref.[8] and the J^π-values are from Refs.[8] and [26] and from the present work. The identification between the experimental and shell-model $J^\pi=0^+_3$ and $J^\pi=3^+_8$ levels is not from this work but from Ref.[26] (see text, subsection V.B). For this reason, these levels are connected by a broken line.

TABLES

TABLE I. Spectroscopic information from the $^{29}Si(d,^3He)^{28}Al$ reaction at 29 MeV.

Ref.[8]		This work					Ref.[6]		
E_x(MeV) [a]	J^π	E_x(MeV) [b]	J^π [c]	C^2S l_p=0	C^2S l_p=1	C^2S l_p=2	C^2S l_p=0	C^2S l_p=1	C^2S l_p=2
0	3^+	0				2.39			
									3.58
0.031	2^+	0.032				1.26			
0.972	0^+	0.971		0.13					
							0.04		0.20
1.014	3^+	1.012				0.10			
1.373	1^+	1.375		0.39			0.47		
1.620	1^+								
		1.624				0.15			0.25
1.623	2^+								
2.139	2^+	2.138				0.42			
									0.60
2.201	1^+	2.201				0.11			
2.272	4^+	2.272 [d]							
2.486	2^+	2.484				0.26			0.27
(2.566)	$(1-3^+)$	[e]							
2.582	5^+	2.578							
2.656	4^+	2.655							<0.1
2.988	$(1,3)^+$	2.986	3^+			0.13			0.36
3.012 ± 4	0^+	3.009		(0.004)					
3.105 ± 1	$(1,3)^+$	3.105	1^+	0.001		0.030			

Table I (*Continued.*)

Ref.[8]		This work					Ref.[6]			
E_x(MeV) [a]	J^π	E_x(MeV) [b]	J^π [c]	C^2S l_p=0	C^2S l_p=1	C^2S l_p=2		C^2S l_p=0	C^2S l_p=1	C^2S l_p=2
3.296	3^+	[f]				0.060	}			
							}			0.19
3.347	2^+	3.348				0.23 [g]	}			
3.465	4^-	3.464								
3.542	1^+	3.542		0.016		0.012		0.09		
3.591	3^-									
		3.601 [h]								
3.671	3^+	[i]				<0.049				
3.709	$(2,3)^+$	3.706				0.073				
3.762 ± 4	$(0)^+$	3.758	0^+	0.031						
3.876	2^-									
3.901	$(1,3,5)^+$	3.900								
3.936	2^+	3.936								
4.033	5^-									
4.115	1^+	4.114		0.012		0.026				
4.244	2^+	4.244				0.072				
4.311 ± 4	$(1,3,5)^+$	4.316								
4.385 ± 4	π nat.									
4.462	$(2,4)^+$ [j]	4.459								

Table I (*Continued.*)

Ref.[8]		This work					Ref.[6]		
E_x(MeV) [a]	J^π	E_x(MeV) [b]	J^π [c]	C^2S l_p=0	C^2S l_p=1	C^2S l_p=2	C^2S l_p=0	C^2S l_p=1	C^2S l_p=2
4.517 ± 4	3^+	4.514							
4.597	$(1,3)^+$ [k]	4.597	3^+			0.044			
4.691	3^-	4.688							
4.739 ± 2	(0^+-5^+)								
4.765	2^-	4.768							
4.846 ± 4	1^+	4.845		0.009		0.065			
4.904	2^-								
4.927 ± 4	π unnat.	4.929							
		4.998 [l]	$(0-2)^-$		0.77			1.10	
4.999 ± 8	2^+								
5.016	3^+								
5.134	3^-								
5.165 ± 2	$6^-(4,5)^-$								
5.177	(1^+-3^+)								
5.188 ± 8									
5.287 ± 4	π nat.								
5.328 ± 8		}							
		} 5.335							
5.343 ± 8		}							

Table I (*Continued.*)

Ref.[8]		This work				Ref.[6]		
E_x(MeV) [a]	J^π	E_x(MeV) [b]	J^π [c]	C^2S l_p=0	C^2S l_p=1	C^2S l_p=2	C^2S l_p=0	C^2S l_p=1	C^2S l_p=2
5.378	(1^+-4^+)	5.377							
5.402 ± 8									
		5.406 [l]	$(0-2)^-$		0.32				
5.442	2^-	5.443							
5.522 ± 8									
5.593 ± 8									
5.741	$(1-4)^+$	5.736							
5.762		5.760							
5.798	2^-	5.800							
5.809									
5.861	$(2,3)^+$	5.857							
5.904	$(1-3)^+$								
5.925									
5.957									
5.981									
5.992	0^+ [m]								
6.005									
6.020	(1^+-4^+)								

Table I (*Continued.*)

Ref.[8]		This work					Ref.[6]		
E_x(MeV) [a]	J^π	E_x(MeV) [b]	J^π [c]	C^2S l_p=0	C^2S l_p=1	C^2S l_p=2	C^2S l_p=0	C^2S l_p=1	C^2S l_p=2
		6.021 [l]	$(0-2)^-$		0.20				
6.064		}							
		} 6.066							
6.071	$(0,1)^+$	}							
6.160									
6.199	(2^+-4^+)								
6.238	$(0-2)^-$								
6.317	2^+	6.317							
6.329		6.335							
6.420		6.422							
6.441		}							
		} 6.451							
6.454		}							
6.462		6.469							
6.481		}							
		} 6.489							
6.493		}							
6.513									
6.564									
6.572									
6.587		6.584							

Table I (*Continued.*)

Ref.[8]		This work					Ref.[6]		
E_x(MeV) [a]	J^π	E_x(MeV) [b]	J^π [c]	C^2S l_p=0	C^2S l_p=1	C^2S l_p=2	C^2S l_p=0	C^2S l_p=1	C^2S l_p=2
6.623	(1^+-4^+)								
6.651	(0^+-3^+)								
		6.652 [l]	$(0-2)^-$		0.20				
6.671									
6.720		6.716							

[a] The excitation energy value of Ref.[8] is rounded off to the nearest keV whenever ΔE_x is less than 1 keV.

[b] All ± 5 keV.

[c] New (or definitely established) J^π-value from this work.

[d] The level at E_x=2.272 MeV in ^{28}Al is mixed at all angles with the ^{27}Al levels at E_x=2.981 and 3.004 MeV, $J^\pi=3/2^+$ and $9/2^+$, respectively.

[e] See text, Section III and subsection V.B.

[f] This level is mixed at all angles with the ^{27}Al level at E_x=4.055 MeV, $J^\pi=1/2^-$, (see text, Section III and subsection V.B).

[g] This C^2S value is obtained with the assumption of a $1d_{3/2}$ transition (see Section IV).

[h] This level is presented as a new level (see Section III).

[i] If this level is populated in this work, it is mixed at all angles with the ^{27}Al level at E_x=4.410 MeV, $J^\pi=5/2^+$, (see text, Section III and subsection V.B).

[j] The $J^\pi=(1\text{-}5)^+$ assignment of Ref.[8] was changed into $J^\pi=(2,4)^+$ in Ref.[26].

[k] The $J^\pi=1^+$ assignment of Ref.[8] was changed into $J^\pi=(1,3)^+$ in Ref.[26].

[l] This level is presented as a new level (see text, subsection V.C).

[m] This level is the first T=2 state in ^{28}Al. Its population through the (d,^{3}He) reaction is therefore isospin-forbidden.

TABLE II. Optical model parameters used in DWBA calculations.

Channel	V (MeV)	r_r (fm)	a_r (fm)	W_V (MeV)	$4W_D$ (MeV)	r_i (fm)	a_i (fm)	$V_{s.o.}$ (MeV)	$r_{s.o.}$ (fm)	$a_{s.o.}$ (fm)	r_c (fm)
^{29}Si + d	85.0	1.17	0.758	1.05	47.6	1.325	0.745	6.49	1.07	0.66	1.30
^{27}Al + ^{3}He	198.4	1.15	0.665	25.4		1.541	0.824				1.40
Proton	[a]	1.25	0.65					λ=25	1.25[b]	0.65[b]	1.25

[a] The depth is adjusted by the code DWUCK4.

[b] DWUCK4 calculations were done also with $r_{s.o.}$=1.00 fm and $a_{s.o.}$=0.52 fm (see text, Section IV).

TABLE III. Comparison of the C^2S values for some states observed in various studies of the $^{28}Si(d,^3He)^{27}Al$ reaction.

E_x[a] (MeV)	J^π	nlj	C^2S This work	C^2S [b]	C^2S [c]	C^2S Shell-model[d]
0	$5/2^+$	$1d_{5/2}$	3.57[e]	3.75	3.40	3.62
0.844	$1/2^+$	$2s_{1/2}$	1.01	0.49	0.79	0.65
1.014	$3/2^+$	$1d_{3/2}$	0.57	0.56	0.48	0.31
2.735	$5/2^+$	$1d_{5/2}$	0.58	0.61	0.41	0.36
4.055	$1/2^-$	$1p_{1/2}$	1.57[f]	1.80	1.51	
4.410	$5/2^+$	$1d_{5/2}$	$\leq$0.42[f]	0.35	0.29	0.24
5.156	$3/2^-$	$1p_{3/2}$	0.84	1.00	1.22	

[a] The excitation energy values from Ref.[8] are rounded off to the nearest keV.

[b] E_d=34.5 MeV, Ref.[21].

[c] E_d=52 MeV, Ref.[6].

[d] Ref.[2].

[e] The C^2S value was fixed to this value in order to determine the number of ^{28}Si nuclei in the target (see text, subsection V.A).

[f] See text, subsection V.B.

TABLE IV. Comparison of the experimental and shell-model predicted values for excitation energy and C^2S in ^{28}Al.

Shell-model						This work				ΔE_x
E_x	J^π_i	C^2S				E_x[a]	J^π[b]	C^2S		(keV)
(MeV)		$2s_{1/2}$	$1d_{3/2}$	$1d_{5/2}$	$l_p=2$	(MeV)		$l_p=0$	$l_p=2$	
0	2^+_1		0.00	1.37	1.37	0.031	2^+		1.26	+ 31
0.142	3^+_1			2.31		0	3^+		2.39	−142
0.840	0^+_1	0.13				0.972	0^+	0.13		+132
0.977	3^+_2			0.035		1.014	3^+		0.10	+ 37
1.364	1^+_1	0.33	0.007			1.373	1^+	0.39		+ 9
1.537	2^+_2		0.067	0.073	0.12	1.623	2^+ }			+ 86
							}		0.15	
1.746	1^+_2	0.001	0.040			1.620	1^+ }			−126
2.073	1^+_3	0.019	0.067			2.201	1^+		0.11	+128
2.102	2^+_3		0.012	0.31	0.31	2.139	2^+		0.42	+ 37
2.436	2^+_4		0.027	0.073	0.093	2.486	2^+		0.26	+ 50
2.895	0^+_2	0.000				3.012	0^+	(0.004)		+117
3.061	3^+_3			0.13		2.988	3^+[c]		0.13	− 24
3.135	2^+_5		0.10	0.014	0.12	3.347	2^+		0.23[d]	+212
3.198	1^+_4	0.007	0.000			3.105[e]	1^+[c]	0.001	0.030	− 93
3.249	3^+_4			0.014		3.296	3^+		0.060	+ 47
3.449	0^+_3	0.017				3.762	0^+[c]	0.031		+313
3.474[f]	3^+_5			0.022		3.671	3^+		<0.048	+197

Table IV (*Continued.*)

Shell-model						This work				ΔE_x
E_x	J^π_i	C^2S				E_x[a]	J^π[b]	C^2S		(keV)
(MeV)		$2s_{1/2}$	$1d_{3/2}$	$1d_{5/2}$	$l_p=2$	(MeV)		$l_p=0$	$l_p=2$	
3.524	1^+_5	0.011	0.003			3.542[g]	1^+	0.016	0.012	+ 18
3.598	3^+_6			0.000						
3.632[h]	2^+_6		0.029	0.001	0.031	3.709	$(2,3)^+$		0.073	+ 77
3.715	2^+_7		0.009	0.023	0.029					
3.876	3^+_7			0.034						
3.925	1^+_6	0.018	0.016			4.115[i]	1^+	0.012	0.026	+190
4.030	2^+_8		0.007	0.042	0.047	4.244	2^+		0.072	+214
4.230	3^+_8			0.016		4.597	3^+[c]		0.044	+367
4.929	1^+_7	0.005	0.009			4.846[j]	1^+	0.009	0.065	− 83
5.160	1^+_8	0.009	0.009							
6.066	0^+_4	0.002								
7.152	0^+_5	0.001								
7.410	0^+_6	0.000								

[a] The excitation energy values from Ref.[8] are rounded off to the nearest keV.

[b] Ref.[8] unless indicated otherwise.

[c] This work (see text, subsection V.2).

[d] This value is obtained with the assumption of a $1d_{3/2}$ transfer.

[e] For this level the value of the parameter $\alpha(=S_{l=0}/(S_{l=0}+S_{l=2}))$ is equal to 0.04 ± 0.01 whereas the shell-model prediction is $\alpha=1.00$.

[f] This level is identified in Ref.[26] with the level at E_x=3.671 MeV, $J^\pi=3^+$, (see text, subsection V.B).

[g] For this level α=0.57±0.05 whereas the shell-model prediction is 0.80.

[h] This level is identified in Ref.[26] with the level at E_x=3.709 MeV, $J^\pi=(2,3)^+$, (see text, subsection V.B).

[i] For this level α=0.32±0.08 whereas the shell-model prediction is 0.53.

[j] For this level α=0.13±0.06 whereas the shell-model prediction is 0.38.

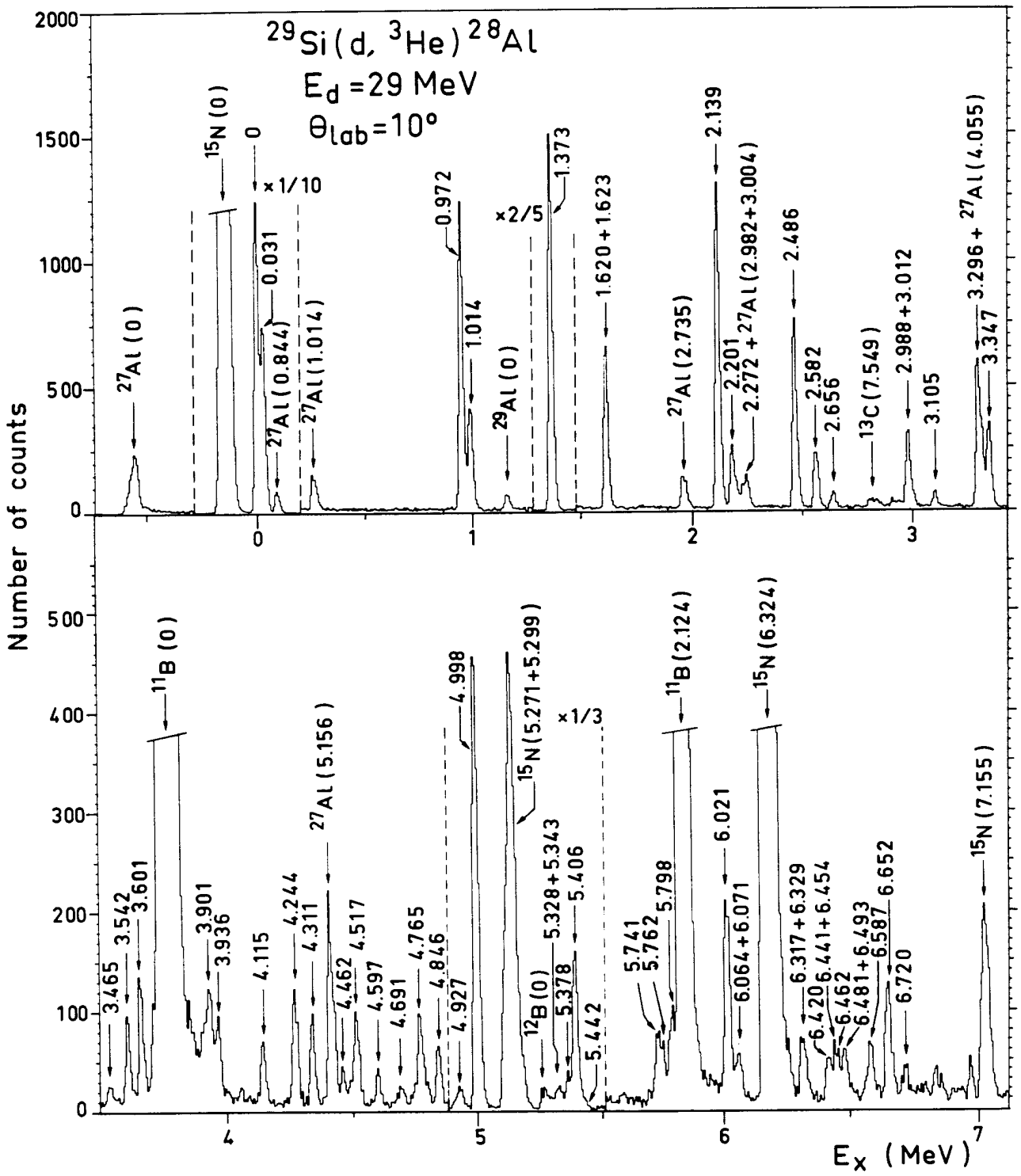
^{29}Si(d, ^{3}He)^{28}Al
E_d =29 MeV
θ_{lab}=10°
Number of counts
E_x (MeV)
^{27}Al (0)
^{15}N (0)
0
×1/10
0.031
^{27}Al (0.844)
^{27}Al (1.014)
0.972
1.014
^{29}Al (0)
×2/5
1.373
1.620+1.623
^{27}Al (2.735)
2.139
2.201
2.272 + ^{27}Al (2.982+3.004)
2.486
2.582
2.656
^{13}C (7.549)
2.988+3.012
3.105
3.296 + ^{27}Al (4.055)
3.347
^{11}B (0)
3.465
3.542
3.601
3.901
3.936
4.115
4.244
4.311
^{27}Al (5.156)
4.462
4.517
4.597
4.691
4.765
4.846
4.927
4.998
^{15}N (5.271+5.299)
×1/3
^{12}B (0)
5.328+5.343
5.378
5.406
5.442
5.741
5.762
5.798
^{11}B (2.124)
6.021
6.064+6.071
^{15}N (6.324)
6.317+6.329
6.420
6.441+6.454
6.462
6.481+6.493
6.587
6.652
6.720
^{15}N (7.155)

Fig. 1

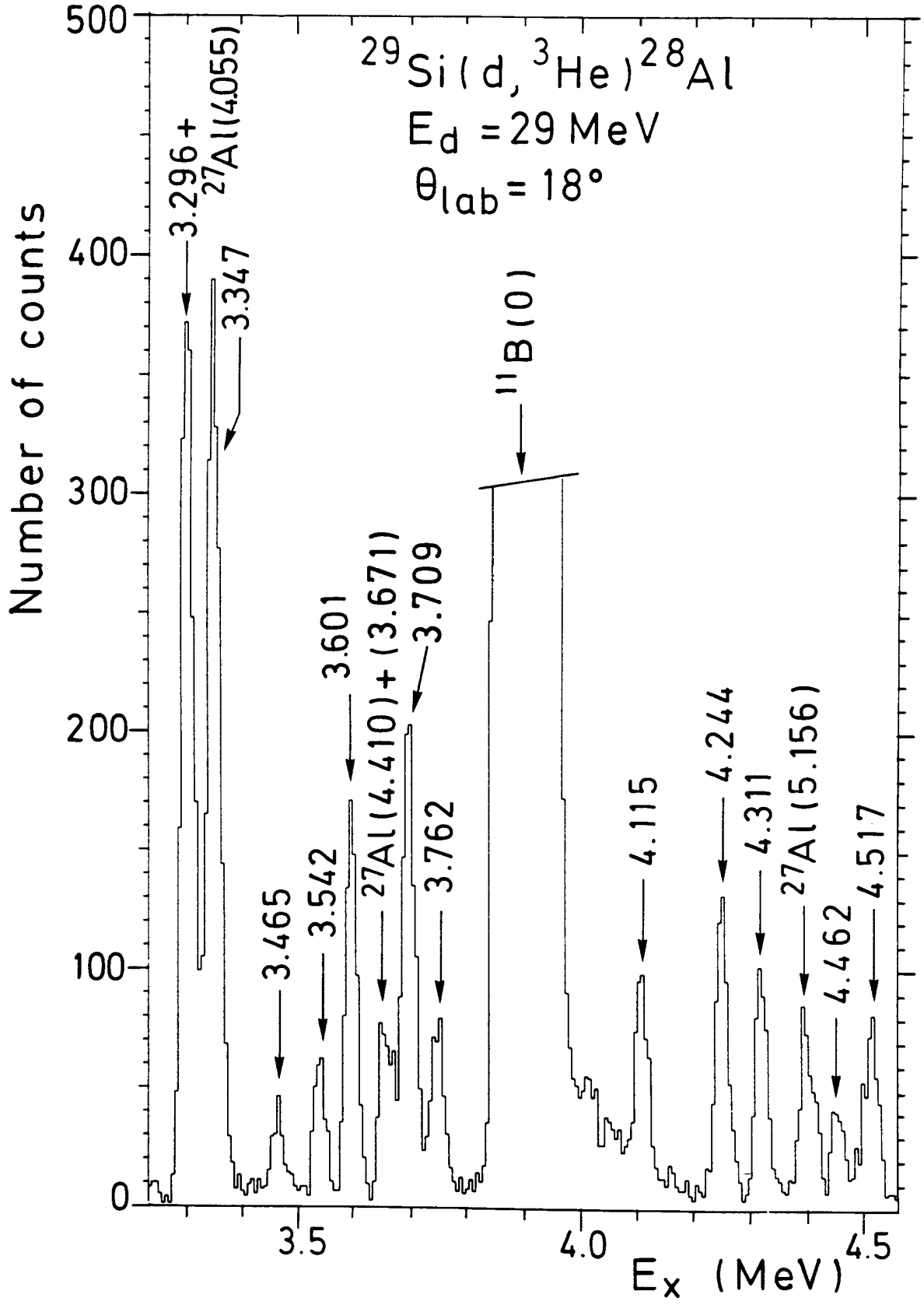
$^{29}Si(d,{}^{3}He)^{28}Al$
$E_d = 29$ MeV
$\theta_{lab} = 18°$
Number of counts
E_x (MeV)
3.296 + ^{27}Al(4.055)
3.347
3.465
3.542
3.601
^{27}Al(4.410) + (3.671)
3.709
3.762
^{11}B(0)
4.115
4.244
4.311
^{27}Al(5.156)
4.462
4.517

Fig. 2

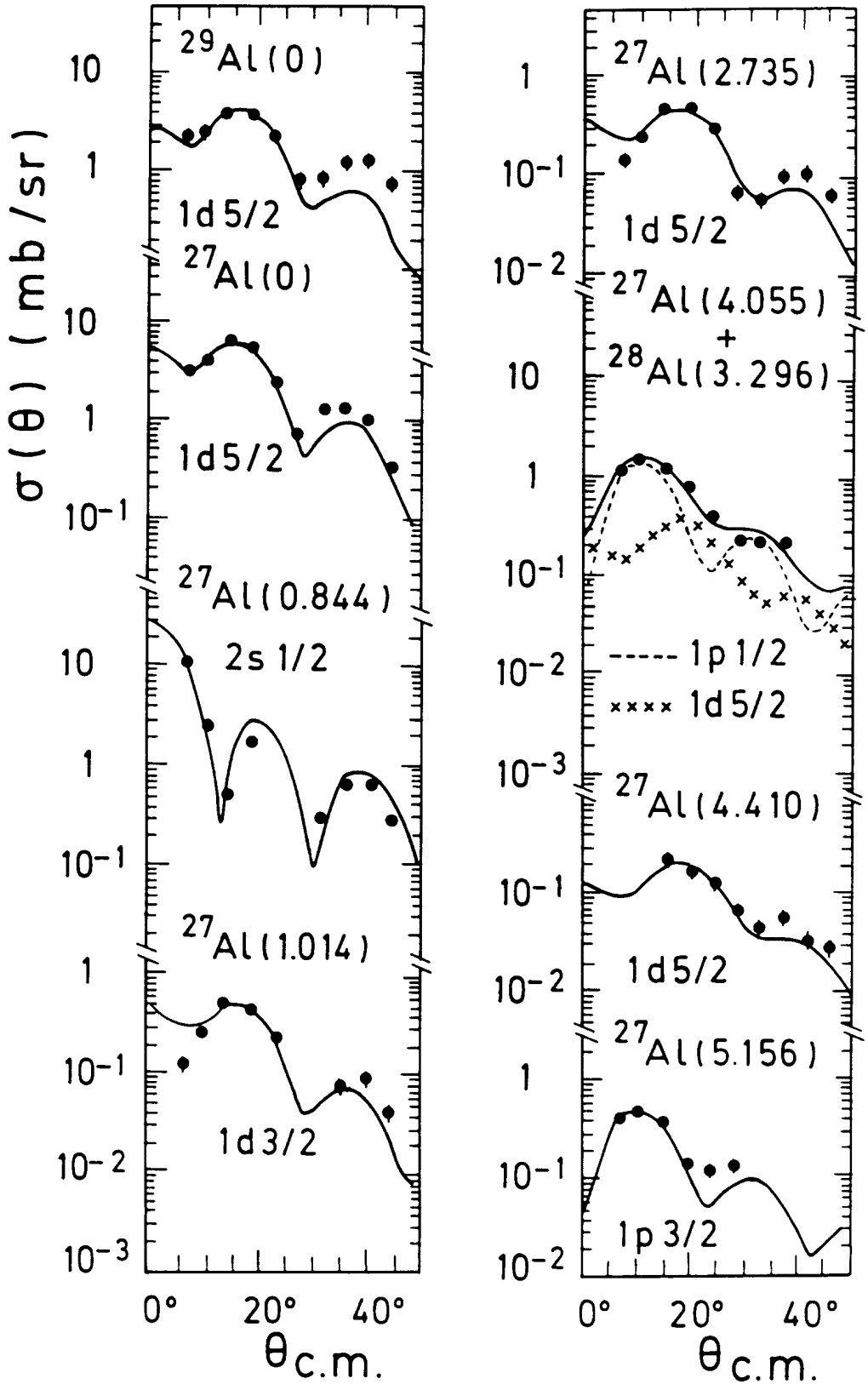
σ(θ) (mb/sr)
29Al(0)
1d5/2
27Al(0)
1d5/2
27Al(0.844)
2s1/2
27Al(1.014)
1d3/2
27Al(2.735)
1d5/2
27Al(4.055)
+
28Al(3.296)
----- 1p1/2
×××× 1d5/2
27Al(4.410)
1d5/2
27Al(5.156)
1p3/2
0°
20°
40°
θc.m.

Fig. 3

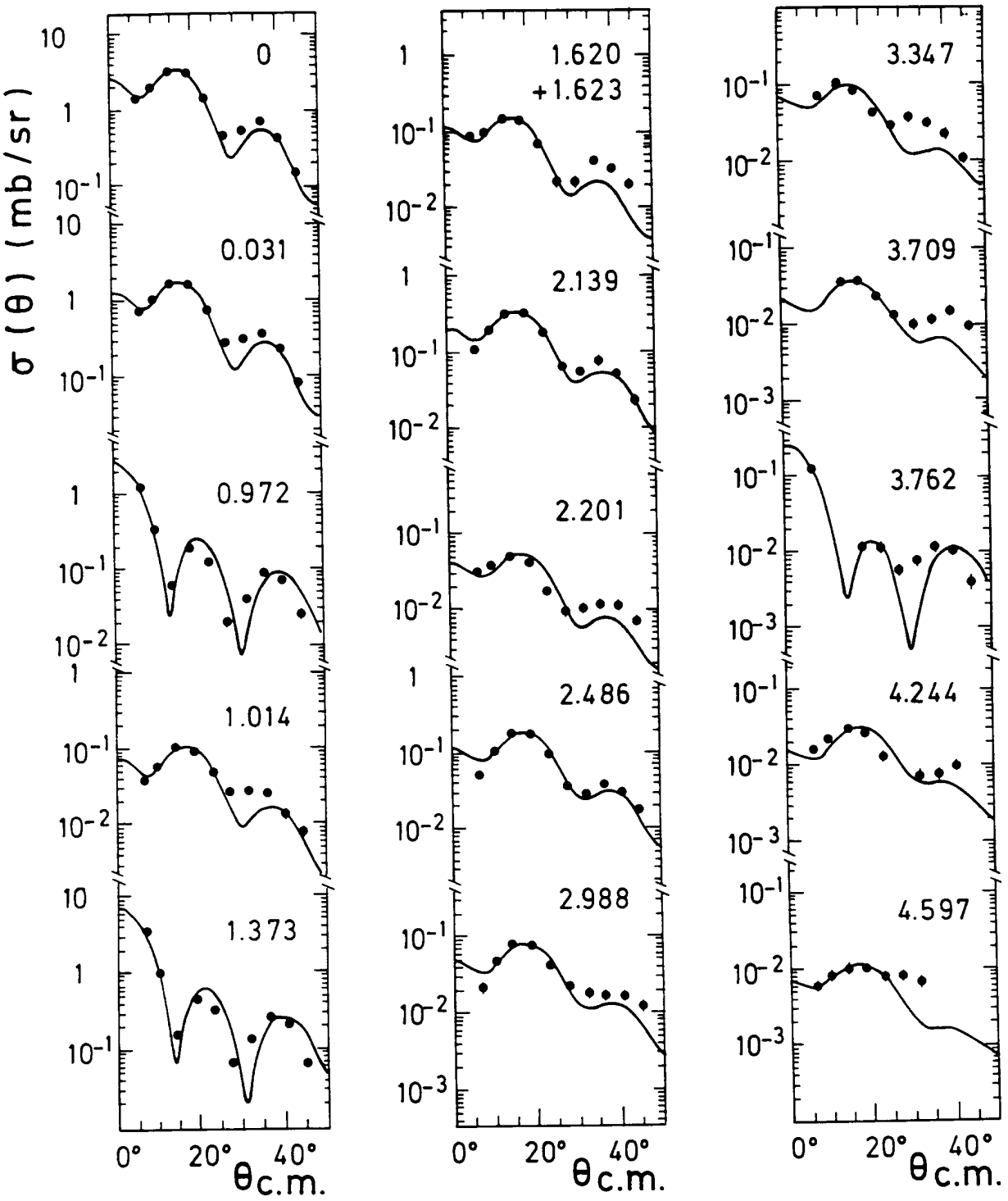
σ (θ) (mb/sr)
0
0.031
0.972
1.014
1.373
1.620
+1.623
2.139
2.201
2.486
2.988
3.347
3.709
3.762
4.244
4.597
0°
20°
40°
θc.m.

Fig. 4

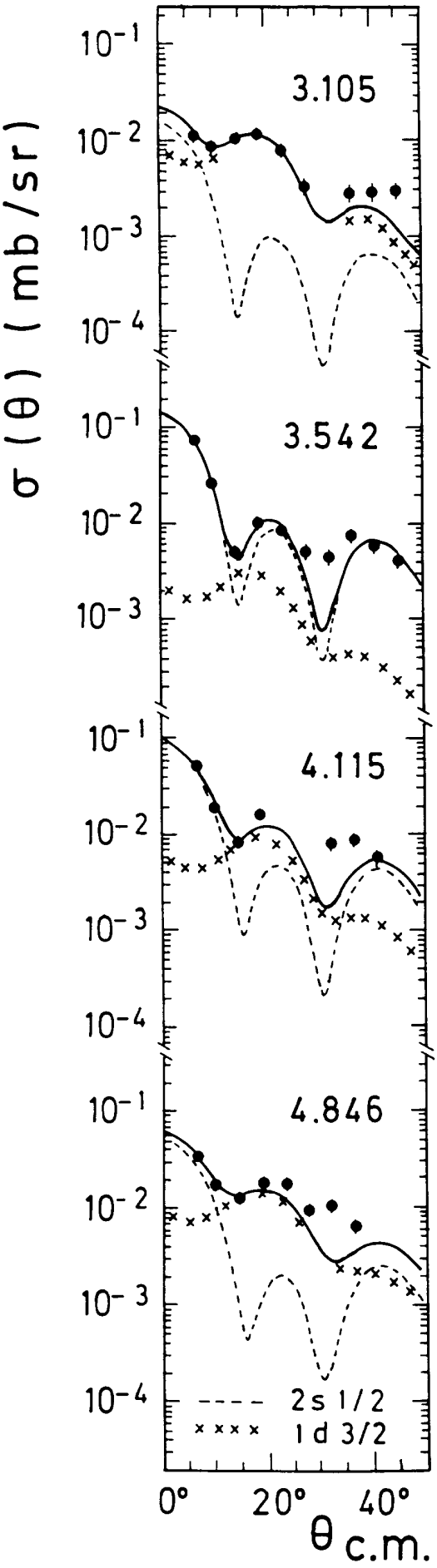
σ (θ) (mb/sr)
10-1
10-2
10-3
10-4
3.105
3.542
4.115
4.846
---- 2s 1/2
×××× 1d 3/2
0°
20°
40°
θ c.m.

Fig. 5

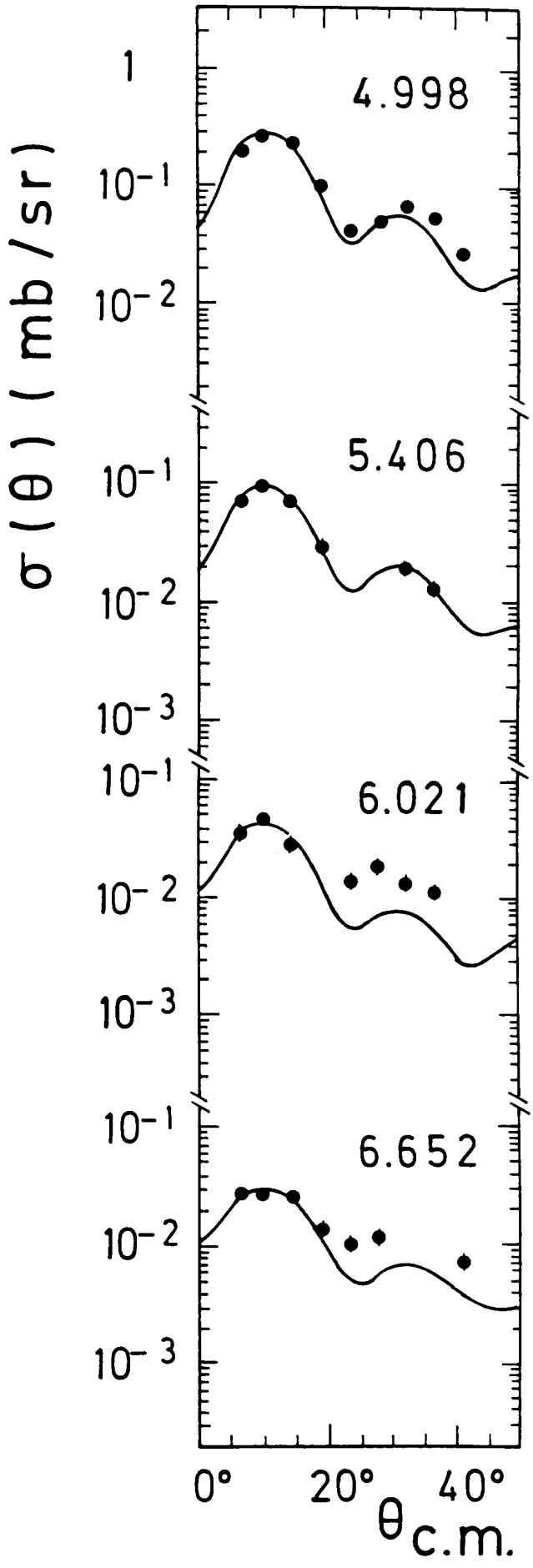
σ(θ) (mb/sr)
1
10⁻¹
10⁻²
4.998
10⁻¹
10⁻²
10⁻³
5.406
10⁻¹
10⁻²
10⁻³
6.021
10⁻¹
10⁻²
10⁻³
6.652
0°
20°
40°
θc.m.

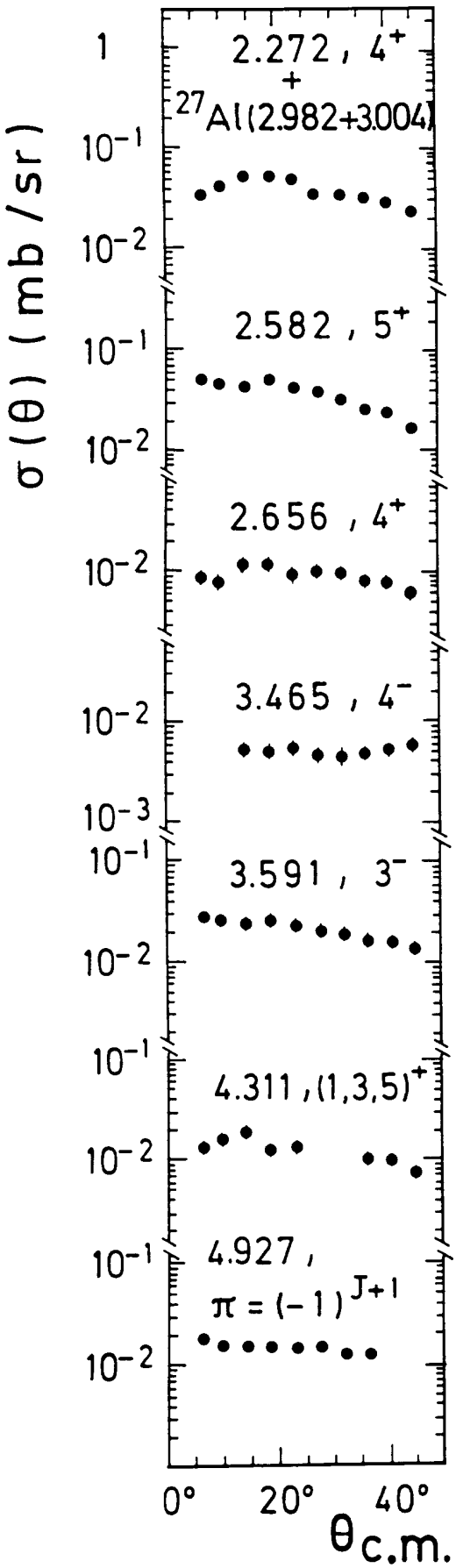
σ(θ) (mb / sr)
1
10⁻¹
10⁻²
10⁻¹
10⁻²
10⁻²
10⁻²
10⁻³
10⁻¹
10⁻²
10⁻¹
10⁻²
10⁻¹
10⁻²
2.272 , 4⁺
+
²⁷Al(2.982+3.004)
2.582 , 5⁺
2.656 , 4⁺
3.465 , 4⁻
3.591 , 3⁻
4.311 , (1,3,5)⁺
4.927 ,
π = (−1)^J+1
0°
20°
40°
θc.m.

Fig. 7

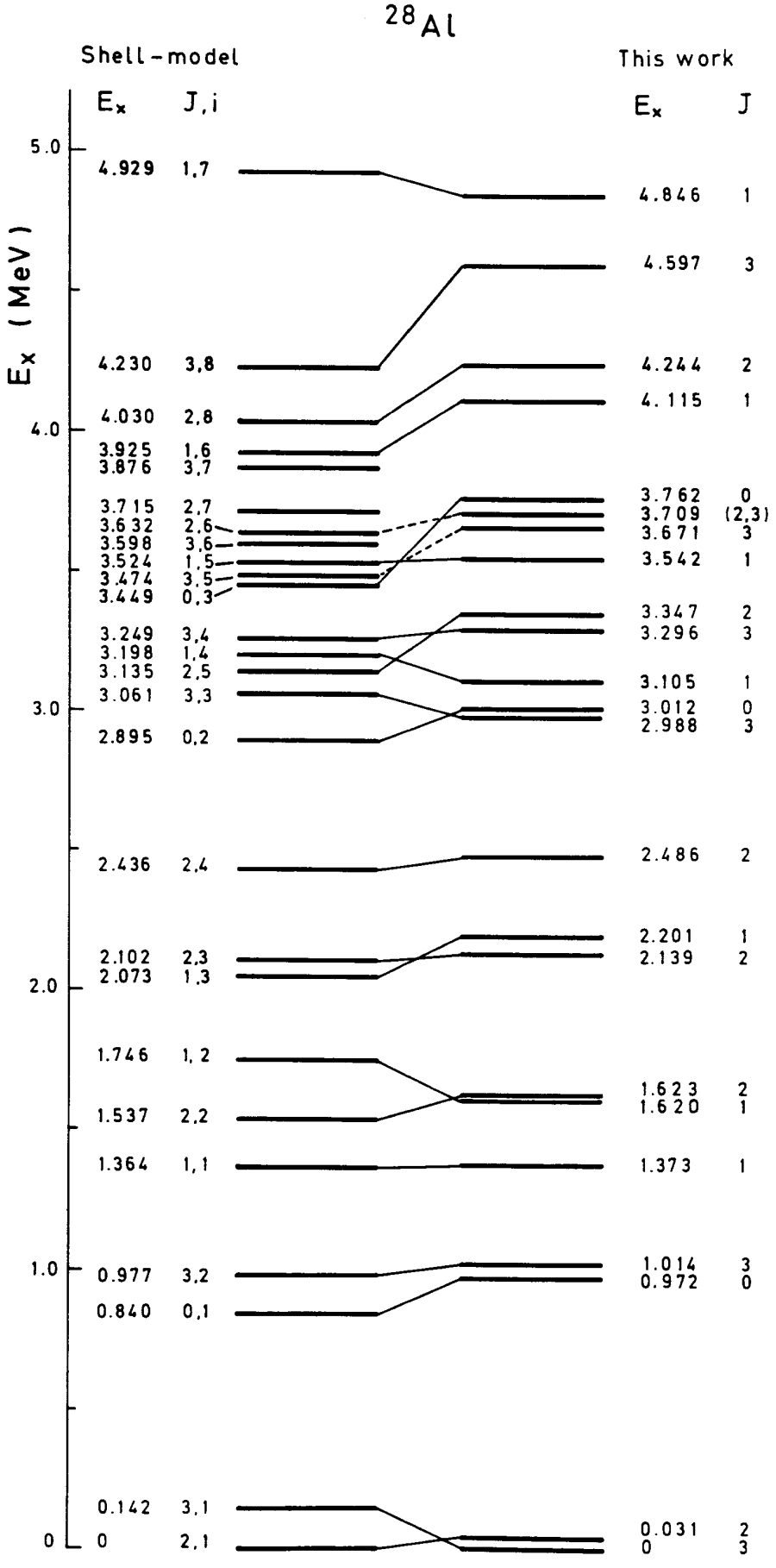
28Al
Shell-model
This work
Ex
J,i
Ex
J
Ex (MeV)
5.0
4.0
3.0
2.0
1.0
0
4.929 1,7
4.230 3,8
4.030 2,8
3.925 1,6
3.876 3,7
3.715 2,7
3.632 2,6
3.598 3,6
3.524 1,5
3.474 3,5
3.449 0,3
3.249 3,4
3.198 1,4
3.135 2,5
3.061 3,3
2.895 0,2
2.436 2,4
2.102 2,3
2.073 1,3
1.746 1,2
1.537 2,2
1.364 1,1
0.977 3,2
0.840 0,1
0.142 3,1
0 2,1
4.846 1
4.597 3
4.244 2
4.115 1
3.762 0
3.709 (2,3)
3.671 3
3.542 1
3.347 2
3.296 3
3.105 1
3.012 0
2.988 3
2.486 2
2.201 1
2.139 2
1.623 2
1.620 1
1.373 1
1.014 3
0.972 0
0.031 2
0 3